Thermal conductivity calculation of nano-suspensions using Green–Kubo relations with reduced artificial correlations

2017 J. Phys.: Condens. Matter 29 155302

(http://iopscience.iop.org/0953-8984/29/15/155302)

IOP Publishing Journal of Physics: Condensed Matter
J. Phys.: Condens. Matter **29** (2017) 155302 (7pp) https://doi.org/10.1088/1361-648X/aa5f08

Thermal conductivity calculation of nano-suspensions using Green–Kubo relations with reduced artificial correlations

Murali Gopal Muraleedharan[1], Dilip Srinivas Sundaram[2], Asegun Henry[3] and Vigor Yang[1]

[1] School of Aerospace Engineering, Georgia Institute of Technology, Atlanta, GA 30332, United States of America
[2] Indian Institute of Technology Gandhinagar, Palaj, Gandhinagar, Gujarat, 382355, India
[3] George W. Woodruff School of Mechanical Engineering, Georgia Institute of Technology, Atlanta, GA 30332, United States of America

E-mail: vigor.yang@aerospace.gatech.edu

Received 3 November 2016, revised 26 January 2017
Accepted for publication 7 February 2017
Published 7 March 2017

Abstract

The presence of artificial correlations associated with Green–Kubo (GK) thermal conductivity calculations is investigated. The thermal conductivity of nano-suspensions is calculated by equilibrium molecular dynamics (EMD) simulations using GK relations. Calculations are first performed for a single alumina (Al_2O_3) nanoparticle dispersed in a water medium. For a particle size of 1 nm and volume fraction of 9%, results show enhancements as high as 235%, which is much higher than the Maxwell model predictions. When calculations are done with multiple suspended particles, no such anomalous enhancement is observed. This is because the vibrations in alumina crystal can act as low frequency perturbations, which can travel long distances through the surrounding water medium, characterized by higher vibration frequencies. As a result of the periodic boundaries, they re-enter the system resulting in a circular resonance of thermal fluctuations between the alumina particle and its own image, eventually leading to artificial correlations in the heat current autocorrelation function (HCACF), which when integrated yields abnormally high thermal conductivities. Adding more particles presents 'obstacles' with which the fluctuations interact and get dissipated, before they get fed back to the periodic image. A systematic study of the temporal evolution of HCACF indicates that the magnitude and oscillations of artificial correlations decrease substantially with increase in the number of suspended nanoparticles.

Keywords: Green–Kubo, molecular dynamics, artificial correlation, periodic boundary conditions, thermal conductivity, nanofluid, autocorrelation

(Some figures may appear in colour only in the online journal)

Introduction

Growing demand for alternative fuels and propellants has led to the development of energetic nano-suspensions with superior burning behaviors [1, 2]. While enhanced chemical reactivity owing to the high specific surface area of nanoparticles helps in achieving better burning characteristics, reduced heat conduction and associated thermal losses may impede their commercialization [3, 4]. Recent studies on the combustion of energetic nano-suspensions suggest that the burning rate is proportional to the square root of the thermal diffusivity of the medium [5, 6]. A 10% enhancement in thermal conductivity, therefore, increases the burning rate by ~5%, resulting in a cleaner and much more efficient combustion.

Molecular dynamics (MD) simulations can be used to predict thermal conductivity, and also to examine the microscopic

nature of heat conduction. Equilibrium MD (EMD) and non-equilibrium MD (NEMD) are the two commonly used techniques. In NEMD, thermal conductivity is determined using Fourier's law of heat conduction [7], wherein a heat flux is imposed on the system and the resulting temperature gradient is calculated; the reverse may also be done, calculating a heat flux from an imposed temperature gradient. In either case, temperature differences greater than ~10 K result in unphysical high heat fluxes and non-linear temperature profiles. Size effects may also be present, as the system must be large enough, in the case of solids, to contain long wavelength and long mean-free-path (MFP) phonons [8]. In EMD, the system is in equilibrium throughout the simulation. EMD is sometimes preferred over NEMD, owing to its lesser size-dependency for solids. System size should be large enough to include all the necessary wavelengths, but not necessarily the MFPs [7, 9, 10], as periodic boundary conditions (PBC) allow phonons to propagate past the boundaries and re-enter through the opposite face without being scattered.

EMD can be combined with the fluctuation-dissipation theorem to calculate thermal conductivity [11]. Here, the linear response of the system to a small thermal perturbation is determined from the time history of the equilibrium fluctuations of the volume averaged heat flux. The thermal conductivity, k, is given by the Green–Kubo (GK) relation as,

$$k = \frac{1}{k_B T^2}\int_0^\infty \frac{\langle \vec{S}(t)\cdot\vec{S}(0)\rangle}{3}\mathrm{d}t, \quad (1)$$

where the heat current vector S was derived by Hardy [12]

$$\vec{S} = \frac{1}{V}\left\{\sum_i \frac{\vec{p}_i}{m_i}\left(\frac{p_i^2}{2m_i}+U_i\right)+\sum_i\sum_i\left(\frac{\partial U_{ij}}{\partial r_i}\cdot\vec{v}_i\right)\vec{r}_{ij}\right\} \quad (2)$$

where V is the volume of the system, T the equilibrium temperature, k_B the Boltzmann constant, p the momentum, v the velocity, and r the position, m the mass, U the potential energy, and summation is over atoms denoted by i. The term in angular brackets represents the heat current autocorrelation function (HCACF). In equation (2), the first term is the convective term and the second is the virial term. In the GK formulation, thermal conductivity depends on the time taken for fluctuations to lose memory of their original values. Studies have shown that fluctuations in crystalline materials are correlated for a longer time, resulting in higher thermal conductivity [8, 13]. Conversely, fluctuations lose correlation quickly in amorphous materials and liquids [14].

For homogeneous systems, equation (2) is sufficient to represent the heat current. However, for multicomponent systems, self-diffusion of species is possible. In order to account for it, the convective term may be corrected with the partial enthalpy [15], h_e of each species a:

$$\vec{S}_{\mathrm{conv}} = \frac{1}{V}\left[\sum_{i=1}^{N}\frac{\vec{p}_i}{m_i}\left(\frac{p_i^2}{2m_i}+U_i\right)-\sum_{a=1}^{n}h_{e,a}\sum_{i=1}^{N_a}\vec{v}_{a,i}\right]. \quad (3)$$

From thermodynamics, enthalpy $H = E + PV$. This can be expressed statistically as:

$$h_{e,a} = \frac{\sum_{i=1}^{N_a}\left[K_i + P_i + \frac{1}{3}\left(m_i\vec{v}_i{}^2 + \frac{1}{2}\sum_{j=1}^{N}\vec{r}_{ij}\cdot\vec{F}_{ij}\right)\right]}{N_a}, \quad (4)$$

where the sum of the first two terms corresponds to the total energy E, and the terms in the brackets represent the PV term. It was shown by Babaei *et al* [16] that the properties of multi-component systems are sensitive to a non-zero h_e, which if not subtracted from convective heat flux can reflect in HCACF, which when integrated, results in anomalous thermal conductivity values.

Numerous studies report thermal conductivity predictions of nanofluids using GK relations [17–25]. Sankar *et al* [19] used a platinum-water nanofluid system with volume fractions (ϕ) in the range of 1–7%. Atomic interactions were modeled using Lennard–Jones (LJ) and Spohr-Heinzinger potentials. Results suggested a 70% enhancement in thermal conductivity at $\phi = 7\%$. A physical explanation was not given, but one possible reason for the high prediction is that the analysis did not consider enthalpy correction. Sarkar *et al* [18] studied a system of 2 nm copper particles in argon fluid using LJ potential to model interactions. An enhancement of 52% was reported for $\phi = 8\%$, which is significantly higher than Maxwell model (26%) [26]; this was attributed to Brownian motion effects. Note that the Maxwell model is based on the effective medium theory (EMT), which assumes a fully dispersed dilute nanofluid with non-interacting suspended nanoparticles. In reality, however, particles can interact and undergo Brownian motion resulting in a stirring effect. Consequently, several modified Maxwell models were developed, and these unusually high thermal conductivity enhancements in MD simulations were credited to Brownian motion effects [27, 28]. Although earlier experimental studies [29, 30] also support this theory, Brownian motion may, however, be not of concern owing to the large timescales associated with particle motion [31, 32].

Another theory that has been proposed to explain the anomalous enhancement is based on the formation of nanolayer around the particle [20, 25, 33]. Nanolayer is believed to function as a high thermal conductivity conduit for interfacial heat flow. Interfacial (Kapitza) resistance, on the other hand, has an opposite effect. Over the last decade, there have been several attempts to include effects of nanolayering and interfacial resistance in classical thermal conductivity models. Yu and Choi [34] developed a modified Maxwell model, by treating particle-nanolayer core–shell complex dispersed in the base-fluid. By judiciously choosing a constant nanolayer thickness of ~2–3 nm and nanolayer thermal conductivity of 10–100 k_f, reasonable agreement with experimental data was achieved. The core–shell complex particle assumption was also used by several other researchers to develop effective thermal conductivity models [35, 36]. These models only yield qualitative descriptions of the variations of effective thermal conductivity with particle volume fraction and particle size. In the GK calculations by Sachdeva *et al* [20] for copper-water nanofluid, an advanced flexible-3-center (F3C) model for water and the finitely extensible nonlinear elastic (FENE) potential for copper were used. Results showed an

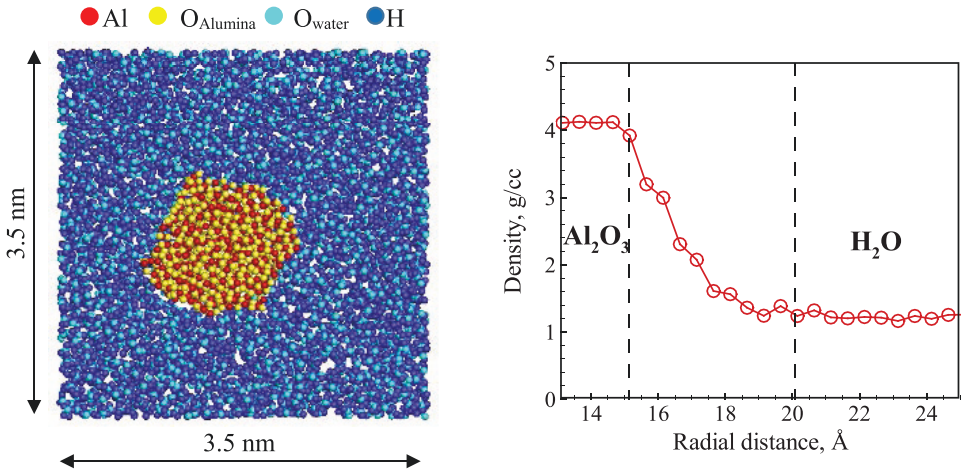

Figure 1. (a) Cross-section of single nanoparticle simulation system, and (b) radial density profile for 1 nm particle suspension at $\phi \sim 1\%$.

enhancement as high as 80% for $\phi = 5\%$ and 1 nm particle. This was attributed to hydration layering on the copper surface. This argument relies on earlier [34] and concurrent [37] experimental investigations favoring nanolayer effects. Yu and Choi [34] attributed an enhancement greater than 40% (for $\phi = 3\%$) solely to nanolayering, whereas, Feng *et al* [37] suggest contributions from both nanolayering and particle aggregation. Recent studies, however, have shown that the thermal conductivity of the adsorbed layer is only marginally greater than that of the base fluid [38, 39]. Taking the high interfacial resistance also into consideration, the nanolayer theory may not conclusively explain the results [40].

It is evident that GK relations often give high thermal conductivity values, but the physical origin of this behavior is elusive. It is counterintuitive to obtain thermal conductivity enhancements for fully-dispersed nanoparticle suspensions higher than the EMT models. Therefore, it is wise to conduct a detailed MD analysis before seeking physical explanations to possible underlying mechanisms. In this work, we conduct systematic EMD simulations using alumina-water nano-suspensions, and calculate the effective thermal conductivity for a range of volume fractions and particle sizes.

Methodology

EMD simulations are conducted for a system consisting of a single alumina (Al_2O_3) nanoparticle and water molecules. GK relations are used to calculate thermal conductivity at a temperature of 300 K. Partial enthalpy correction is applied. Volume fraction is in the range 1–10%. Particle sizes of 1 and 3 nm are considered. Note that when the particle size is changed, simulation cell size is readjusted to obtain the target volume fraction. Atomic interactions within Al_2O_3 are modeled using the potential function developed by Vashishta *et al* [41]. Interactions in water are captured using the extended simple point charge [42] (SPC/E) model, with bonds constrained by the SHAKE algorithm [43]. Long-range electrostatic interactions are treated by particle-particle-particle-mesh (pppm) summation [42]. The alumina-water cross-interaction is modeled using Lorentz-Berthelot rules [44], where $\varepsilon_{Al-Al} = 1.4383 \times 10^{-8}$ eV, $\sigma_{Al-Al} = 5.3814$ Å, $\varepsilon_{O-O} = 1.6847 \times 10^{-3}$ eV, and $\sigma_{O-O} = 3.9883$ Å [45].

The nanoparticle and water systems are independently equilibrated at the target temperature. For the water system, isobaric-isothermal (NPT) ensemble is used and PBC are imposed in all three directions. Temperature and pressure were controlled by Nose–Hoover thermostat and barostat, respectively. For nanoparticles, microcanonical (NVE) ensemble is used, and free boundary conditions are imposed on all directions. Berendsen thermostat [46] is used to maintain the temperature of the nanoparticle at 300 K. The suspension is created by creating a spherical cavity at the center of the water domain and inserting the equilibrated nanoparticle in the cavity. Care was taken to make sure that there is no overlap of atomic positions. The box dimension is chosen based on the volume fraction, while ensuring that densities of both materials match the experimental counterparts. After the particle and water systems are independently equilibrated, they are combined, as shown in figure 1(a). The resulting system is equilibrated at 300 K and 1 bar in Nose–Hoover isobaric-isothermal (NPT) ensemble for 100 ps using a time step of 0.1 fs. The thermal conductivity calculation is then carried out for a time period of 5 ns; heat current correlation times are in the range 2.5–10 ps. All simulations are conducted using the LAMMPS [47] MD code; the velocity verlet algorithm is used for time-integration.

Results and discussion

Figure 2 shows the variation of effective thermal conductivity (k_e/k_f) of the mixture with volume fraction (ϕ). Results suggest a near-linear variation of k_e/k_f with ϕ, aligning well with the behavior of nanofluids [48]. For a particle size of 3 nm and $\phi \sim 9$ %, k_e/k_f is ~200%, substantially greater than the predictions of the nanofluid thermal conductivity models. As particle size is reduced to 1 nm, the enhancement increases to 235% at $\phi \sim 9\%$. This is similar to the observations of other researchers [20]. In the absence of aggregation or Brownian motion, enhancements may be credited to possible nanolayer effects, and the hypothesis can be tested. In essence, the

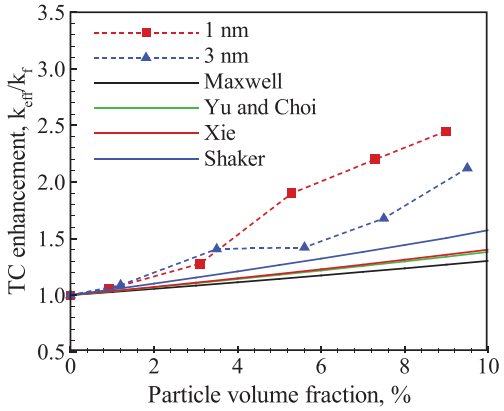

Figure 2. Enhancement in effective thermal conductivity (TC) as a function of particle volume fraction compared with various thermal conductivity models.

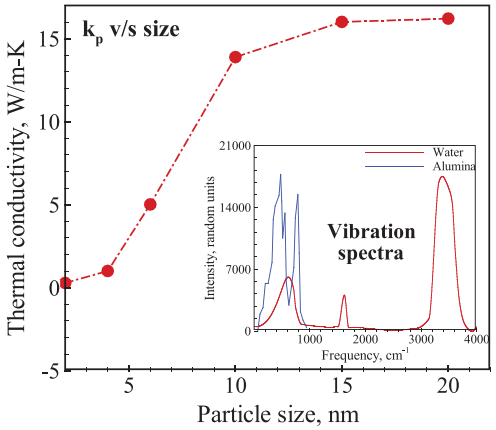

Figure 3. Thermal conductivity of alumina nanoparticle as a function of particle size; *Inset*: comparison of vibrational spectra of alumina and water.

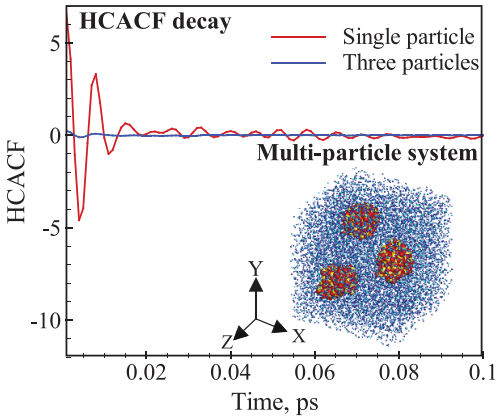

Figure 4. Time decay of heat current autocorrelation function 1 nm particle, $\phi = 10\%$; *Inset*: multi-particle simulation system.

nanolayer thickness, h, may be estimated using a radial density profile, as shown in figure 1(b), evaluated using 0.5–1 Å thick spherical shells around the particle. The nanolayer can be approximately taken as the region between the particle surface and the shell in which the density reduces to the bulk density of water. For the cases in figure 2, the estimated nanolayer thickness is ~6.5–9 Å or 2–3 atomic layers, and it is independent of the particle size. This is in agreement with the physisorption theory [49] as well as with *ab initio* findings [50]. As a result, smaller particles may be expected to have a higher relative nanolayer thickness, h/D, resulting in a higher thermal conductivity, producing a seemingly convincing validation of the nanolayer hypothesis.

This hypothesis, however, has several pitfalls. Firstly, as seen in figure 1(a), the nanoparticle is not a perfect sphere. Surface roughness, with a characteristic dimension of a few angstroms, could contribute to an increase in mass density near the surface. Furthermore, water layering occurs mainly by hydrogen bonding, which does not cause significant density changes [51], as reported in other works [20, 25]. In addition, the NEMD analysis of Liang *et al* [38] suggests that the nanolayer thermal conductivity is only ~1.6 times that of the liquid, suggesting its insignificant role in interfacial conduction.

The size effect on thermal conductivity also poses concerns. Figure 3 shows the effect of particle size on thermal conductivity, k_p, of alumina nanoparticles. For a 1 nm particle, k_p is only about one-fifteenth of the bulk value. This is expected, as the phonon MFP decreases with decreasing particle size due to boundary scattering [52] and accessible phonon modes are limited due to size-restricted phonon wavelengths. This suggests that the effective thermal conductivity of nanofluids may decrease with decreasing particle size, contrary to the trend shown in figure 2.

To resolve the contradiction, two factors governing the calculated thermal conductivity are inspected: magnitude of the HCACF, and the time required for the fluctuations to lose correlation. If the correlations are large and/or remain intact for a long time, greater thermal conductivity may be expected. As periodic boundary conditions are imposed, it is possible that an atom will experience perturbations from its own periodic image. Particularly, an atom can thus experience an artificial enhancement in the self-correlated heat current, as its motion perturbs the surrounding atoms, and then be transmitted through the entire supercell back to itself. The returning and initial perturbations are likely to be well-correlated, as they originate from the same atom. This is unrealistic because every atom is unique, and perturbations to its surrounding environment can never possess a circular resonance with its own motion. The observed thermal conductivity enhancement could thus simply be a numerical artefact arising from the periodic boundary conditions.

Disparities in vibrational frequencies may also play an important role in exacerbating this problem. Comparison of the vibration spectra of alumina and water [41, 53], as shown in figure 3 (inset), reveals that the frequencies associated with water are 3–4 times higher than that of alumina. Consequently, water would experience vibrations of alumina atoms as low frequency sound waves. As lower frequency waves can be transmitted farther through a medium, Al_2O_3 vibrations have a greater propensity to establish a circular resonance. These perturbations can thus form a feedback loop if they are not sufficiently damped by the surrounding water molecules; this will be accentuated in smaller simulation domains and/or systems with long-range forces, such as those in ionic suspensions. For

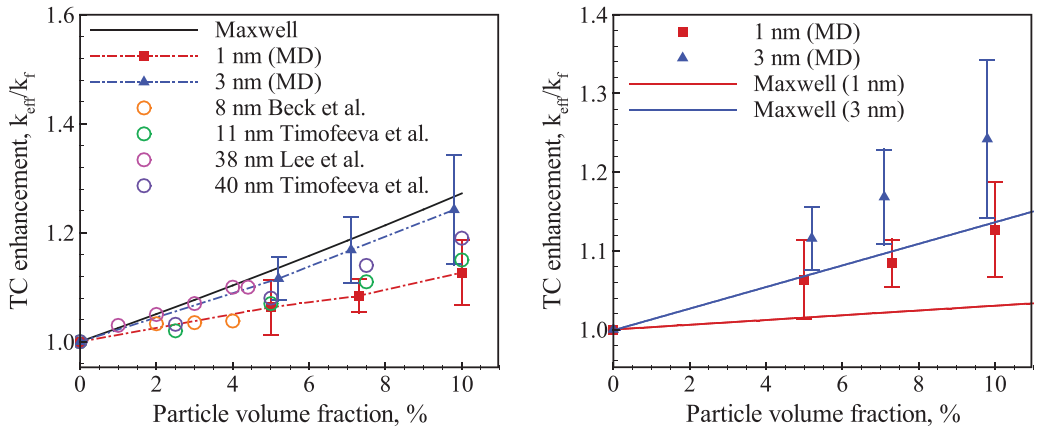

Figure 5. Enhancement in effective thermal conductivity (TC) calculated from multi-particle simulations as a function of particle volume fraction compared with (a) Maxwell model [26] with bulk thermal conductivity of alumina and experimental results [55, 56]. (b) Maxwell model with thermal conductivity of alumina particles from figure 3.

the alumina-water system, the electrostatic part of the SPC/E force-field is truncated at 10 Å, whereas the Vashishta *et al* [41] potential is truncated at 6 Å. For a 1 nm particle suspension, however, the minimum distance between an alumina atom and its nearest image is only ~4 Å, which is insufficient to prevent contamination of HCACF statistics with unrealistic self-correlations. As the particle size and volume fraction increases, the system gets larger and self-interactions and artificial correlations are suppressed.

This is an intrinsic problem associated with GK calculations; the problem could be mitigated by choosing a system size large enough to minimize artificial correlations. This, however, imposes constraints on the maximum attainable volume fraction with single-nanoparticle, although volume fractions as high as 20–30% are of concern for many practical propulsion and energy-conversion systems. Alternatively, we may use multiple nanoparticles in the system, as illustrated in figure 4 (inset). It is logical to expect that the addition of more nanoparticles is likely to hamper the development of artificial self-correlations due to the presence of unrelated perturbations from other nanoparticles, thereby breaking the symmetry that a single particle tries to establish with its own image. This hypothesis is tested by comparing the time decay of HCACF for single and three-particle systems, as shown in figure 4. For single-particle systems, HCACF oscillates substantially before decaying to zero. These fluctuations are, however, damped in three-particle systems, resulting in a quicker and smoother decay. Prior studies attributed these oscillations to back-scattering of phonons at the particle-fluid interface [54] or to the relative motion of dissimilar atoms [13]. Results of the present study, however, suggest that the oscillations are merely associated with artificial correlations.

Thermal conductivity is then recalculated for multi-particle supercells. By gradually increasing the particle count and testing for convergence, it was found that a minimum of three alumina particles are required to diminish statistical errors. Multiple initial configurations were used to remove any directional dependencies, and an average of twelve independent runs were used to calculate thermal conductivity. Figure 5 shows the resulting variation of k_{eff}/k_f with ϕ for different particle sizes. MD predictions are compared with experimental results [55, 56] and the Maxwell model. In figure 5(a), bulk thermal conductivity is used, while in figure 5(b), nanoparticle thermal conductivity (from figure 3) is used. Experimental data correspond to nanofluids with negligible aggregation. Results do not suggest any anomalous enhancement beyond the Maxwell model. In fact, MD predictions are lower than the Maxwell model, and agree well with the experimental data. Furthermore, the effective thermal conductivity also increases with increasing particle size, which is consistent with the size dependent thermal conductivity behavior of nanoparticles. Figure 5(b) shows that MD predictions are marginally greater than Maxwell model predictions using nanoparticle thermal conductivity values. This may be because the Vashishta potential underestimates the thermal conductivity of alumina, as explained earlier.

Conclusions

To conclude, an alternative explanation to the unusually high thermal conductivity of nano-suspensions obtained using Green–Kubo relations is provided. While prior studies credit them to dynamic heat transport mechanisms, our results suggest that these high values are merely an outcome of artificial correlations, arising from single nanoparticle systems and periodic boundary conditions, thereby contaminating the heat current autocorrelation function (HCACF). This problem is expected to be prominent for systems in which vibration frequencies of the constituents are disparate. In such cases, low frequency perturbations are transmitted through the surrounding high frequency medium and return to the originating particle due to periodic boundary conditions. The resulting circular resonance contaminates the HCACF, which is more pronounced for smaller particles and/or higher volume fractions. In an effort to alleviate this artifact, multi-particle systems are considered. The presence of additional particles impedes the development of artificial self-correlations by breaking the particle-image symmetry. Thermal conductivity predicted from the rectified HCACF is in good agreement with experimental data and the Maxwell model predictions. It

is to be noted that the required minimum number of particles depends on the simulation system, which can be determined by devising an appropriate convergence test.

Acknowledgments

This work was sponsored by the Air force Office of Scientific Research under contract no. FA-9550-13-1-0004. The support and encouragement provided by Dr Mitat A Birkan is gratefully acknowledged.

References

[1] Sabourin J L *et al* 2009 Functionalized graphene sheet colloids for enhanced fuel/propellant combustion *ACS Nano* **3** 3945–54
[2] Risha G A *et al* 2007 Combustion of nano-aluminum and liquid water *Proc. Combust. Inst.* **31** 2029–36
[3] Rossi C *et al* 2007 Nanoenergetic materials for MEMS: a review *IEEE/ASME J. Microelectromech. Syst.* **16** 919–31
[4] Taylor R *et al* 2013 Small particles, big impacts: a review of the diverse applications of nanofluids *J. Appl. Phys.* **113** 011301
[5] Sundaram D S and Yang V 2014 Effect of packing density on flame propagation of nickel-coated aluminum particles *Combust. Flame* **161** 2916–23
[6] Sundaram D S *et al* 2013 Effects of particle size and pressure on combustion of nano-aluminum particles and liquid water *Combust. Flame* **160** 2251–9
[7] Schelling P K, Phillpot S R and Keblinski P 2002 Comparison of atomic-level simulation methods for computing thermal conductivity *Phys. Rev.* B **65** 144306
[8] McGaughey A and Kaviany M 2004 Thermal conductivity decomposition and analysis using molecular dynamics simulations. Part I. Lennard–Jones argon *Int. J. Heat Mass Transf.* **47** 1783–98
[9] Henry A S and Chen G 2008 Spectral phonon transport properties of silicon based on molecular dynamics simulations and lattice dynamics *J. Comput. Theor. Nanosci.* **5** 141–52
[10] Henry A and Chen G 2008 High thermal conductivity of single polyethylene chains using molecular dynamics simulations *Phys. Rev. Lett.* **101** 235502
[11] Kubo R 1966 The fluctuation-dissipation theorem *Rep. Prog. Phys.* **29** 255
[12] Hardy R J 1963 Energy-flux operator for a lattice *Phys. Rev.* **132** 168
[13] McGaughey A and Kaviany M 2004 Thermal conductivity decomposition and analysis using molecular dynamics simulations: part II. Complex silica structures *Int. J. Heat Mass Transf.* **47** 1799–816
[14] Evans W, Fish J and Keblinski P 2007 Thermal conductivity of ordered molecular water *J. Chem. Phys.* **126** 154504
[15] Eapen J, Li J and Yip S 2007 Mechanism of thermal transport in dilute nanocolloids *Phys. Rev. Lett.* **98** 028302
[16] Babaei H, Keblinski P and Khodadadi J M 2012 Equilibrium molecular dynamics determination of thermal conductivity for multi-component systems *J. Appl. Phys.* **112** 054310
[17] Wu X, Kumar R and Sachdeva P 2005 Calculation of thermal conductivity in nanofluids from atomic-scale simulations *ASME 2005 Int. Mechanical Engineering Congress and Exposition* (American Society of Mechanical Engineers)
[18] Sarkar S and Selvam R P 2007 Molecular dynamics simulation of effective thermal conductivity and study of enhanced thermal transport mechanism in nanofluids *J. Appl. Phys.* **102** 074302
[19] Sankar N, Mathew N and Sobhan C 2008 Molecular dynamics modeling of thermal conductivity enhancement in metal nanoparticle suspensions *Int. Commun. Heat Mass Transf.* **35** 867–72
[20] Sachdeva P and Kumar R 2009 Effect of hydration layer and surface wettability in enhancing thermal conductivity of nanofluids *Appl. Phys. Lett.* **95** 223105
[21] Kang H, Zhang Y and Yang M 2011 Molecular dynamics simulation of thermal conductivity of Cu–Ar nanofluid using EAM potential for Cu–Cu interactions *Appl. Phys.* A **103** 1001–8
[22] Mohebbi A 2012 Prediction of specific heat and thermal conductivity of nanofluids by a combined equilibrium and non-equilibrium molecular dynamics simulation *J. Mol. Liq.* **175** 51–8
[23] Lin Y-S, Hsiao P-Y and Chieng C-C 2012 Thermophysical characteristics of ethylene glycol-based copper nanofluids using nonequilibrium and equilibrium methods *Int. J. Therm. Sci.* **62** 56–60
[24] Loulijat H *et al* 2015 Effect of Morse potential as model of solid–solid inter-atomic interaction on the thermal conductivity of nanofluids *Adv. Powder Technol.* **26** 180–7
[25] Lee S *et al* 2016 Molecular dynamic simulation: studying the effects of Brownian motion and induced micro-convection in nanofluids *Numer. Heat Transf.* A **69** 643–58
[26] Maxwell J C 1991 *A treatise on Electricity and Magnetism* vol 1 (Oxford: Clarendon)
[27] Prasher R, Bhattacharya P and Phelan P E 2005 Thermal conductivity of nanoscale colloidal solutions (nanofluids) *Phys. Rev. Lett.* **94** 025901
[28] Chon C H *et al* 2005 Empirical correlation finding the role of temperature and particle size for nanofluid (Al_2O_3) thermal conductivity enhancement *Appl. Phys. Lett.* **87** 3107
[29] Das S K *et al* 2003 Temperature dependence of thermal conductivity enhancement for nanofluids *J. Heat Transf.* **125** 567–74
[30] Li C H and Peterson G 2006 Experimental investigation of temperature and volume fraction variations on the effective thermal conductivity of nanoparticle suspensions (nanofluids) *J. Appl. Phys.* **99** 084314
[31] Keblinski P, Prasher R and Eapen J 2008 Thermal conductance of nanofluids: is the controversy over? *J. Nanopart. Res.* **10** 1089–97
[32] Babaei H, Keblinski P and Khodadadi J 2013 A proof for insignificant effect of Brownian motion-induced micro-convection on thermal conductivity of nanofluids by utilizing molecular dynamics simulations *J. Appl. Phys.* **113** 084302
[33] Muraleedharan M G, Sundaram D S and Yang V 2016 Heat transport in aqueous suspensions of alumina nanoparticles *54th AIAA Aerospace Sciences Meeting*
[34] Yu W and Choi S 2003 The role of interfacial layers in the enhanced thermal conductivity of nanofluids: a renovated Maxwell model *J. Nanopart. Res.* **5** 167–71
[35] Leong K, Yang C and Murshed S 2006 A model for the thermal conductivity of nanofluids–the effect of interfacial layer *J. Nanopart. Res.* **8** 245–54
[36] Xie H *et al* 2003 Nanofluids containing multiwalled carbon nanotubes and their enhanced thermal conductivities *J. Appl. Phys.* **94** 4967–71
[37] Feng Y *et al* 2007 The effective thermal conductivity of nanofluids based on the nanolayer and the aggregation of nanoparticles *J. Phys. D: Appl. Phys.* **40** 3164
[38] Liang Z and Tsai H-L 2011 Thermal conductivity of interfacial layers in nanofluids *Phys. Rev.* E **83** 41602
[39] Xue L *et al* 2004 Effect of liquid layering at the liquid–solid interface on thermal transport *Int. J. Heat Mass Transf.* **47** 4277–84

[40] Xue L *et al* 2003 Two regimes of thermal resistance at a liquid–solid interface *J. Chem. Phys.* **118** 337–9
[41] Vashishta P *et al* 2008 Interaction potentials for alumina and molecular dynamics simulations of amorphous and liquid alumina *J. Appl. Phys.* **103** 083504
[42] Mark P and Nilsson L 2001 Structure and dynamics of the TIP3P, SPC, and SPC/E water models at 298 K *J. Phys. Chem.* A **105** 9954–60
[43] Miyamoto S and Kollman P A 1992 SETTLE: an analytical version of the SHAKE and RATTLE algorithm for rigid water models *J. Comput. Chem.* **13** 952–62
[44] Allen M P and Tildesley D J 1989 *Computer Simulation of Liquids* (Oxford: Oxford University Press)
[45] Cygan R T, Liang J-J and Kalinichev A G 2004 Molecular models of hydroxide, oxyhydroxide, and clay phases and the development of a general force field *J. Phys. Chem.* B **108** 1255–66
[46] Hünenberger P H 2005 *Thermostat Algorithms for Molecular Dynamics Simulations, in Advanced Computer Simulation* (Berlin: Springer) pp 105–49
[47] Plimpton S 1995 Fast parallel algorithms for short-range molecular dynamics *J. Comput. Phys.* **117** 1–19
[48] Das S K *et al* 2007 *Nanofluids: Science and Technology* (New York: Wiley)
[49] Ross S and Winkler W 1955 On physical adsorption: IX. Sub-critical and subpracritical adsorption isotherms for krypton monolayers on graphitized carbon black *J. Colloid Sci.* **10** 330–7
[50] Shapovalov V and Truong T N 2000 *Ab initio* study of water adsorption on α-Al_2O_3 (0 0 0 1) crystal surface *J. Phys. Chem.* B **104** 9859–63
[51] Argyris D *et al* 2011 Molecular dynamics studies of interfacial water at the alumina surface *J. Phys. Chem.* C **115** 2038–46
[52] Zhang Z M 2007 *Nano/Microscale Heat Transfer* (New York: McGraw-Hill)
[53] Bernath P F 2002 The spectroscopy of water vapour: experiment, theory and applications *Phys. Chem. Chem. Phys.* **4** 1501–9
[54] Keblinski P *et al* 2002 Mechanisms of heat flow in suspensions of nano-sized particles (nanofluids) *Int. J. Heat Mass Transf.* **45** 855–63
[55] Timofeeva E V *et al* 2007 Thermal conductivity and particle agglomeration in alumina nanofluids: experiment and theory *Phys. Rev.* E **76** 061203
[56] Beck M P *et al* 2009 The effect of particle size on the thermal conductivity of alumina nanofluids *J. Nanopart. Res.* **11** 1129–36